Are there any narrow K^--nuclear states?

J. Hrtánková + J. Mareš

Nuclear Physics Institute, Řež

PLB 770 (2017) 342; PRC 96, 015205 (2017).

EXA 2017, Wien, 10 - 15 September, 2017

The speaker selected by EXA organizers (left) and the corresponding author (right).

- Self-consistent calculations of K^--nuclear quasi-bound states using the following chiral meson-baryon interaction models:
  - Prague (P)
    (A. Cieply, J. Smejkal, Nucl. Phys. A 881 (2012) 115)
  - Kyoto-Munich (KM)
    (Y. Ikeda, T. Hyodo and W. Weise, Nucl. Phys. A 881 (2012) 98)
  - Murcia (M1 and M2)
    (Z. H. Guo and J. A. Oller, Phys. Rev. C 87 (2013) 035202)
  - Bonn (B2 and B4)
    (M. Mai and U.-G. Meiner, Nucl. Phys. A 900 (2013) 51)

Model

- Klein-Gordon equation for K^-

$$\left[\tilde{\omega}_K^2 + \vec{\nabla}^2 - m_K^2 - \Pi_K(\vec{p}_K, \omega_K, \rho)\right] \phi_K = 0 \ ,$$

where complex energy $\tilde{\omega}_K = m_K - B_K - \mathrm{i}\Gamma_K/2 - V_C = \omega_K - V_C$

- Self-energy operator

$$\Pi_K = 2\mathrm{Re}(\omega_{K^-}) V_{K^-}^{(1)} = -4\pi \left(F_0 \tfrac{1}{2}\rho_p + F_1 \left(\tfrac{1}{2}\rho_p + \rho_n\right)\right) ,$$

F_0 and F_1 – isospin 0 and 1 in-medium scattering amplitudes (in the K^--nucleus frame) derived from a chiral meson-baryon interaction model

- Nucleus described within an RMF model
- Static self-consistent calculations

core polarization effects up to $\simeq 5$ MeV in K^- binding energies

(D. Gazda, J. Mareš, Nucl. Phys. A 881 (2012) 159)

Free-space $K^- p$ amplitudes

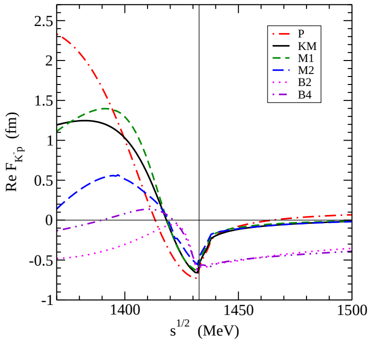

Fig.1: Energy dependence of real (left) and imaginary (right) parts of free-space $K^- p$ amplitudes in considered models.

Free-space $K^- n$ amplitudes

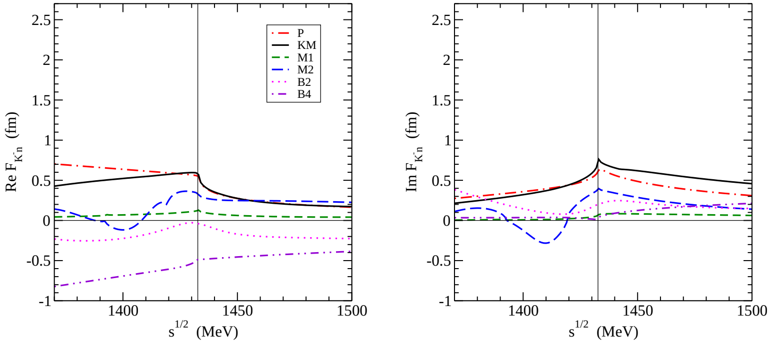

Fig.2: Energy dependence of real (left) and imaginary (right) parts of free-space $K^- n$ amplitudes in considered models.

In-medium $K^- N$ amplitudes

- Free space amplitudes $\rightarrow$ in-medium amplitudes - WRW method
  (T. Wass, M. Rho, W. Weise, Nucl. Phys. A 617 (1997) 449)

$$F_1 = \frac{\frac{\sqrt{s}}{m_N} F_{K^-n}(\sqrt{s})}{1 + \frac{1}{4}\xi_k \frac{\sqrt{s}}{m_N} F_{K^-n}(\sqrt{s})\rho} , \quad F_0 = \frac{\frac{\sqrt{s}}{m_N}[2F_{K^-p}(\sqrt{s}) - F_{K^-n}(\sqrt{s})]}{1 + \frac{1}{4}\xi_k \frac{\sqrt{s}}{m_N}[2F_{K^-p}(\sqrt{s}) - F_{K^-n}(\sqrt{s})]\rho}$$

where $\quad \xi_k = \frac{9\pi}{p_f^2} 4 \int_0^\infty \frac{dt}{t} \exp(iqt) j_1^2(t), \qquad q = \frac{1}{p_f}\sqrt{\omega_{K^-}{}^2 - m_{K^-}^2}.$

- P + Pauli + SE model
  (A. Cieply, J. Smejkal, Nucl. Phys. A 881 (2012) 115)

$$F_{ij}(p, p'; \sqrt{s}) = -\frac{g_i(p) g_j(p')}{4\pi f_i f_j} \sqrt{\frac{M_i M_j}{s}} \left[(1 - C(\sqrt{s}) \cdot G(\sqrt{s})^{-1}) \cdot C(\sqrt{s}) \right]_{ij} ,$$

$$G_i(\sqrt{s}; \rho) = \frac{1}{f_i^2} \frac{M_i}{\sqrt{s}} \int_{\Omega_i(\rho)} \frac{d^3\vec{p}}{(2\pi)^3} \frac{g_i^2(p)}{p_i^2 - p^2 - \Pi_i(\sqrt{s}, \vec{p}; \rho) + i0} .$$

In-medium modified $\bar{K}N$ *amplitudes*

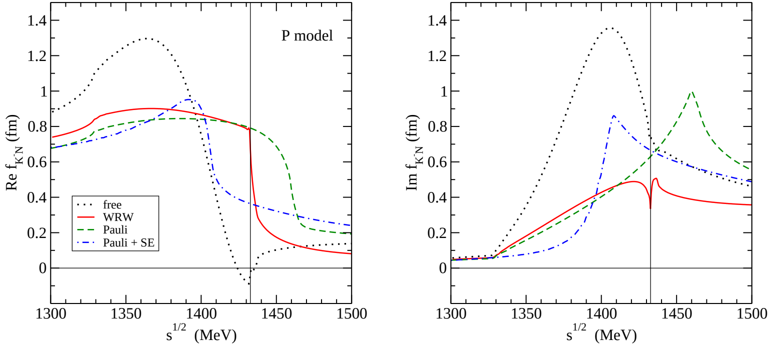

Fig.3: Energy dependence of reduced free-space (dotted line) $f_{K^-N} = \frac{1}{2}(f_{K^-p} + f_{K^-n})$ amplitude compared with WRW modified amplitude (solid line), Pauli (dashed line), and Pauli + SE (dot-dashed line) modified amplitude for $\rho_0 = 0.17\ \mathrm{fm}^{-3}$ in the P model.

In-medium modified $\bar{K}N$ amplitudes

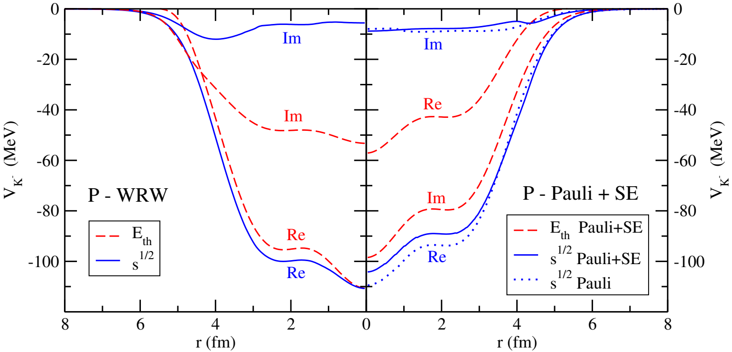

Fig.4: K^- nuclear potential in ^{40}Ca calculated using K^-N P amplitudes at threshold (dashed lines) and with $\sqrt{s}$ (solid lines), in two in-medium versions: WRW (left panel) and including Pauli blocking and hadron self-energies (right panel).

Energy dependence

- K^-N amplitudes are a function of $\sqrt{s}$
  $(s = (E_N + E_{K^-})^2 - (\vec{p}_N + \vec{p}_{K^-})^2)$
- K^-N cms frame $\rightarrow$ K^--nucleus frame $\vec{p}_N + \vec{p}_{K^-} \neq 0$
  (A. Cieplý, E. Friedman, A. Gal, D. Gazda, J. Mareš, PLB 702 (2011) 402)

$$\sqrt{s} = E_{th} - B_N \frac{\rho}{\bar{\rho}} - \xi_N \left[B_{K^-} \frac{\rho}{\rho_{max}} + 23 \left(\frac{\rho}{\bar{\rho}}\right)^{2/3} + V_C \left(\frac{\rho}{\rho_{max}}\right)^{1/3} \right] + \xi_{K^-} \mathrm{Re} V_{K^-}(r) \ ,$$

where $B_N = 8.5$ MeV and $\xi_{N(K^-)} = m_{N(K^-)}/(m_N + m_{K^-})$;
Low-density limit $\delta\sqrt{s} \rightarrow 0$ as $\rho \rightarrow 0$, where $\delta\sqrt{s} = \sqrt{s} - E_{th}$.

- B_{K^-} and V_{K^-} $\Rightarrow$ self-consistency scheme

Energies probed in the calculations

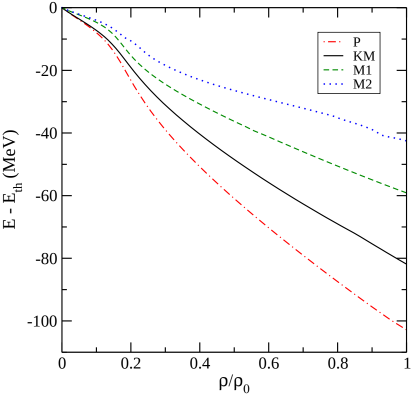

Fig.5: Subthreshold energies probed in the $^{16}O+K^-$ nucleus as a function of relative density ρ/ρ_0, calculated self-consistently using K^-N amplitudes in the P, KM, M1, and M2 models.

K^- 1s binding energies and widths

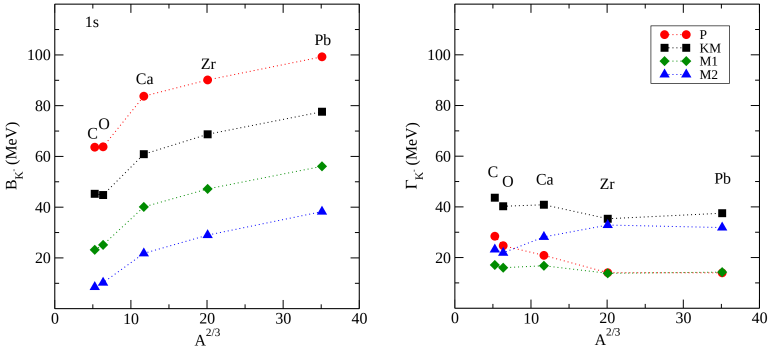

Fig.6: 1s K^- binding energies (left) and corresponding widths (right) in various nuclei calculated self-consistently in the P, KM, M1, and M2 models.

Multinucleon processes

- K^- interactions with two and more nucleons - recent analysis of kaonic atom data including branching ratios of K^- absorption by Friedman and Gal *(NPA 959 (2017) 66)*

$$2\mathrm{Re}(\omega_{K^-})V^{(2)}_{K^-} = -4\pi B(\frac{\rho}{\rho_0})^{\alpha}\rho \ , \quad (1)$$

where B is a complex amplitude and α is positive

- ImB multiplied by a kinematical suppression factor to account for phase space reduction

Multinucleon processes

Table 1: Values of the complex amplitude B and exponent α used to evaluate $V^{(2)}_{K^-}$ for all meson-baryon interaction models considered in this work.

	P1	KM1	P2	KM2
α	1	1	2	2
ReB (fm)	-1.3±0.2	-0.9±0.2	-0.5±0.6	0.3±0.7
ImB (fm)	1.5±0.2	1.4±0.2	4.6±0.7	3.8±0.7
	B2	B4	M1	M2
α	0.3	0.3	0.3	1
ReB (fm)	2.4±0.2	3.1±0.1	0.3±0.1	2.1±0.2
ImB (fm)	0.8±0.1	0.8±0.1	0.8±0.1	1.2±0.2

- Only P and KM models found acceptable by the F+G analysis
  (NPA 959 (2017) 66)

Multinucleon processes

- Experiments with kaonic atoms probe the K^- optical potential (mainly its imaginary part) up to $\sim 50\%$ of ρ_0

$$\Downarrow$$

- We consider two limiting cases for $V_{K^-}^{(2)}$ in our calculations:

  - full density option (FD) – form (1) in the entire nucleus
  - half density limit (HD) – fix $V_{K^-}^{(2)}$ at constant value $V_{K^-}^{(2)}(0.5\rho_0)$ for $\rho(r) \geq 0.5\rho_0$

- Total K^- optical potential $V_{K^-} = V_{K^-}^{(1)} + V_{K^-}^{(2)}$

Total K^- optical potential

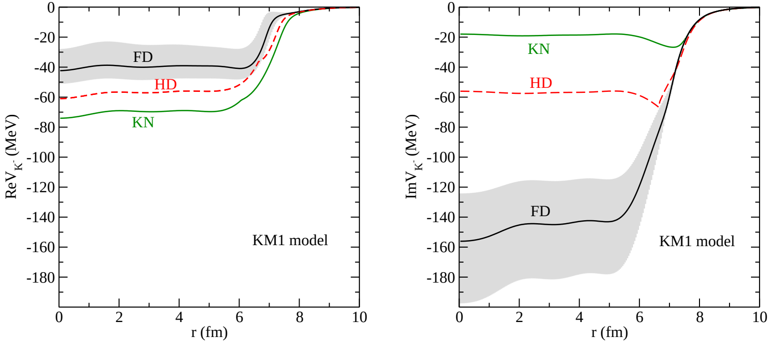

Fig.7: The real (left) and imaginary (right) parts of the K^- optical potential in ^{208}Pb, calculated self-consistently in the KM1 model, for two versions of the K^- multinucleon potential. The shaded area stands for uncertainties. The single-nucleon K^- potential (KN, green solid line) calculated in the KM model is shown for comparison.

Contributions to the total K^- optical potential

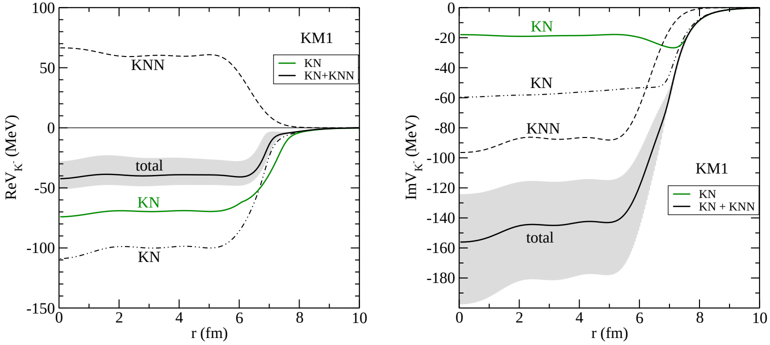

Fig.8: The respective contributions from K^-N and K^-NN potentials to the total real and imaginary K^- optical potential in the ^{208}Pb$+K^-$ nucleus, calculated self-consistently in the KM1 model and FD variant. The single-nucleon K^- potential (green solid line) calculated in the KM model is shown for comparison.

Ratios of K^- absorption in ^{208}Pb

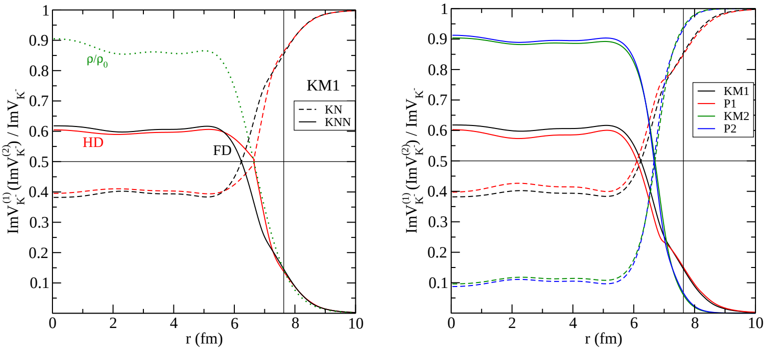

Fig.9: Ratios of $\mathrm{Im}\,V^{(1)}_{K^-}$ and $\mathrm{Im}\,V^{(2)}_{K^-}$ potentials to the total $\mathrm{Im}\,V_{K^-}$ as a function of radius, calculated self-consistently for ^{208}Pb+K^- system in the KM1 model and different option for the K^- multinucleon potential (left) and the comparison of these ratios calculated in different meson-baryon interaction models for FD option (right). The vertical lines denoting $\sim 15\%$ of ρ_0 are shown for comparison.

K^- 1s binding energies and widths

Table 2: 1s K^- binding energies B_{K^-} and widths Γ_{K^-} (in MeV) in various nuclei calculated using the single nucleon K^-N amplitudes (denoted KN); plus a phenomenological amplitude $B(\rho/\rho_0)^\alpha$, where $\alpha = 1$ and 2, for the HD and FD options.

KM model			$\alpha = 1$		$\alpha = 2$	
		KN	HD	FD	HD	FD
^{16}O	B_{K^-}	45	34	not	48	not
	Γ_{K^-}	40	109	bound	121	bound
^{40}Ca	B_{K^-}	59	50	not	64	not
	Γ_{K^-}	37	113	bound	126	bound
^{208}Pb	B_{K^-}	78	64	33	80	53
	Γ_{K^-}	38	108	273	122	429
P model			$\alpha = 1$		$\alpha = 2$	
^{16}O	B_{K^-}	64	49	not	63	not
	Γ_{K^-}	25	94	bound	117	bound
^{40}Ca	B_{K^-}	81	67	not	82	not
	Γ_{K^-}	14	95	bound	120	bound
^{208}Pb	B_{K^-}	99	82	36	96	47
	Γ_{K^-}	14	92	302	117	412

Conclusions

- Calculations of K^--nuclear quasi-bound states in various nuclei
- K^- single-nucleon potentials based on chiral meson-baryon interaction models:
  - large model dependence of K^- binding energies
  - relatively narrow K^- widths
- K^- multinucleon interactions inside the nucleus included:
  - K^- nuclear quasi-bound states in many-body systems, if they ever exist, have huge widths, considerably exceeding their binding energies

Acknowledgements

Thank you Aleš Cieplý, Eli Friedman, and Avraham Gal!